Discontinuous Galerkin Time Domain Methods for Acoustics and Comparison with Finite Difference Time Domain Methods

Xin Wang

Trip Annual Meeting

Jan 29, 2010

Outline

Outline

Seismic wave equations

- acoustic wave equations (pressure-velocity) read

$$\rho(\mathbf{x})\frac{\partial \mathbf{v}}{\partial t} + \nabla p = 0$$
$$\frac{1}{\kappa(\mathbf{x})}\frac{\partial p}{\partial t} + \nabla \cdot \mathbf{v} = f(\mathbf{x}, t; \mathbf{x}_s)$$

- elastic wave equations (pressure-stress) read

$$\rho\frac{\partial v_i}{\partial t} = \sum_j \frac{\partial \sigma_{ij}}{\partial x_j} + f_i \qquad \Leftarrow \quad \text{conservation of momentum}$$
$$\frac{\partial \sigma_{ij}}{\partial t} = \sum_{k,l} \frac{c_{ijkl}}{2}\left(\frac{\partial v_k}{\partial x_l} + \frac{\partial v_l}{\partial x_k}\right) \quad \Leftarrow \quad \text{Hooke's law}$$

p = acoustic pressure, σ_{ij} = stress tensors, $\mathbf{v} = \{v_i\}$ = particle velocity, $\rho(\mathbf{x})$ =mass density, $\kappa(\mathbf{x})$ =bulk modulus, $c_{ijkl}(\mathbf{x})$ = elastic tensor coefficients, $f_i(\mathbf{x}, t)$ = body force

2D acoustic wave equations (pressure-velocity)

$$\frac{\partial q}{\partial t} + A\frac{\partial q}{\partial x} + B\frac{\partial q}{\partial z} = [0, 0, w(t)\delta(\mathbf{x} - \mathbf{x}_s)]^T \ (+i.c.'s, b.c.'s)$$

$$q = \begin{bmatrix} u \\ v \\ p \end{bmatrix}, \quad A = \begin{bmatrix} 0 & 0 & 1/\rho(\mathbf{x}) \\ 0 & 0 & 0 \\ \kappa(\mathbf{x}) & 0 & 0 \end{bmatrix}, \quad B = \begin{bmatrix} 0 & 0 & 0 \\ 0 & 0 & 1/\rho(\mathbf{x}) \\ 0 & \kappa(\mathbf{x}) & 0 \end{bmatrix}$$

- easy to prepare parameters (ρ, κ)
- analytic solutions for convergence tests are accessible, e.g., homogeneous medium, two-layer media
- fewer implementation issues $\Rightarrow$ objective comparison

Numerical methods (time domain wave-field)

FDTD methods

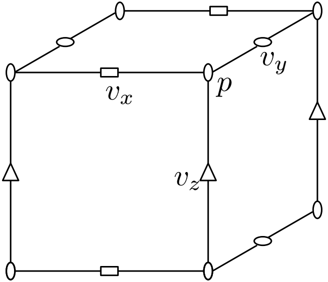

✓ industry standard

✓ easy implementation

✓ desirable balance: efficiency and accuracy

two approaches:

- conventional-grid: lead to numerical instabilities for material parameters with high contrast discontinuities
  reference: *Alford et al., '74*
- staggered-grid: better numerical performance and widely used recently; may lead to interface error
  reference: *Virieux, '84, '86*
  e.g., 4 grids for 3D pressure-velocity acoustic wave equations

Numerical methods (time domain wave-field)

DGTD methods

- specialize in hyperbolic PDEs
- capable of handling complex geometries (boundaries and interfaces)
- explicit semi-discrete form for time dependent PDEs
- high order accuracy: $o(h^{p+1})$ for Cartesian grids, $o(h^{p+1/2})$ for general grid
  reference: *Lesaint and Raviart, ‘74; Johnson and Pitkaranta, ‘86*
- very active in computational electromagnetic and fluid dynamics communities
  reference: *Cockburn and Shu, ‘89; Warburton, ‘99; Käser and Dumbser, ’06*

goal of this project

- apply FDTD and DGTD methods to seismic modeling problems
  - DGTD: implementation based on MIDG developed by Warburton
  - FDTD: staggered-grid FDTD code *iwave* by Terentyev, Vdovina and Symes

- make comparison as objective as possible: measure the CPU time and/or the number of floating point operations for two solutions to roughly have the same accuracy

Outline

Outline

DGTD and FDTD Comparison

true solutions not accessible $\Rightarrow$ **Richardson extrapolation** for error estimation

- assuming the numerical solution $D(h)$ differs from the analytic solution $\bar{D}$ by $E(h) = Ch^p + O(h^{p+1})$, then

$$E(h) \simeq \frac{D(2h) - D(h)}{2^p - 1}$$

- p can be estimated by having $E(2h)$,

$$p \simeq \log_2 \frac{E(2h)}{E(h)}$$

hardware and system (courtesy of Dr. Warburton)

- single precision floating point
- 2.66GHz Intel Core2 Quad Q9450 CPU
- Linux 2.6.18 kernel
- GNU C compiler version 4.1.2

Square-circle model

- computation domain: $[-500\ \mathrm{m}, 500\ \mathrm{m}] \times [-500\ \mathrm{m}, 500\ \mathrm{m}]$
- radius of the circle: 125 m
- inside the circle: $\rho = 1000\ kg/m^3, c = 1000\ m/s$
- outside the circle: $\rho = 1500\ kg/m^3, c = 2000\ m/s$
- a point source "$\bigtriangledown$" at $(0, 250\ m)$
- 41 receivers "$\triangle$" at the depth $-250\ m$, from $-400\ m$ to $400\ m$ at interval of $20\ m$.
- time span: $[0, 2s]$, traces sampled at temporal interval of $5\ ms$.

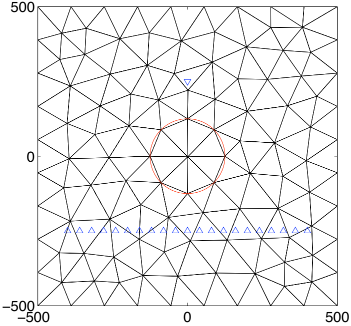

Comparison for square-circle model

2-4 staggered-grid FDTD

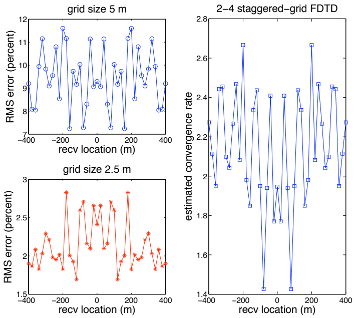

- 33.2 GFLOP, 19 sec
- 2.5 m grid, $\mathrm{CFL} = 0.4$
- 3% RMS error

DGTD, $N = 4$

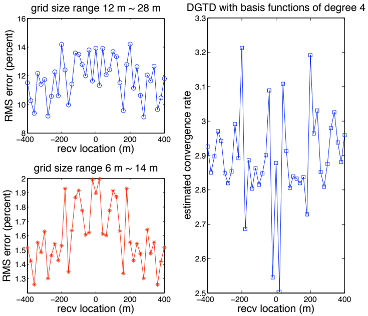

- 2465 GFLOP, 760 sec
- grid size range 6 $\sim$ 14 m, 12,572 eles
- 2% RMS error

2D dome model

- point source with Ricker pulse at $(3300\ \mathrm{m}, 40\ \mathrm{m})$
- significant energy at 30 Hz or a wavelength of 50 m
- receiver at $(2300, 20)$m depth, 3 sec

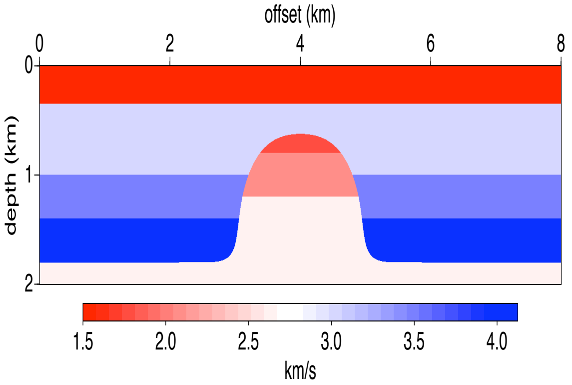

Figure: material wave speed

Comparison for 2D dome model

	2-4 staggered-grid FDTD			DGTD ($N = 2$)	
grid size	1.25 m	0.625 m	0.3125 m	$5 \sim 15$m	$2.7 \sim 7.3$m
0.7-1.1 s	4.64%	1.65%	0.82%	6.11%	0.31%
1.1-1.3 s	12.30%	5.54%	2.76%	5.31%	0.60%
1.5-1.7 s	20.06%	9.45%	4.70%	6.72%	0.79%
1.9-2.1 s	28.64%	13.92%	6.91%	7.23%	1.15%
# GFLOP	1.03e+4	8.22e+4	6.57e+5	1.29e+4	1.03e+5
time	4125 s	32778 s	261991 s	6457 s	52401 s

By extrapolation

- DGTD, N=2: 2.24e+4 GFLOP for 5% RMS error (2nd order)
- 2-4 staggered-grid FDTD: 1.65e+6 GFLOP on 0.23 m grid for the same accuracy (1st order)

Outline

Interface error

Symes & Terentyev & Vdovina '08 report, using staggered FDTD

- Richardson extrapolation estimates of relative RMS errors for 3D dome model ($\Delta x = 5$ m) in various window:
  - 0.7-1.1 s: 20%
  - 1.1-1.3 s: 51%
  - 1.5-1.7 s: 88%
  - 1.9-2.1 s: 120%(!)

e.g., Brown '84, Symes & Vdovina '09
numerical error associated with staggered-grid FDTD of wave propagation in heterogeneous media

- higher order component corresponding to the truncation error
- a first-order error due to the misalignment between numerical grids and material interfaces (time shift)

Interface error

high order convergence rate are expected for DGTD by

- fitting grid points with the interfaces, i.e., interfaces approximated by segments
  - full order convergence for straight-line interfaces
  - 2nd order convergence for curved interfaces ($N > 1$)
- local mesh refinement (h-adaptation) near the interfaces, i.e., decreasing the time shift effect
  reference: *SPICE project*

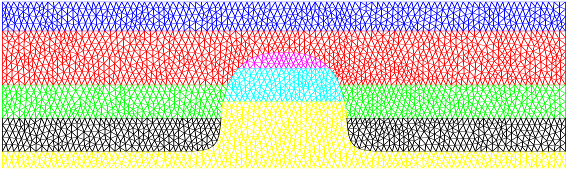

interface fitting mesh for dome model

Plane Wave: Ricker's wavelet

- two different material in $[0, 1800\ m] \times [-15\ m, 15\ m]$
- interface at $x = 900$ m
- misaligned mesh:

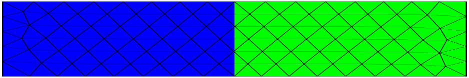

traces of the true and numerical solutions at 500 m, $h = 10\ m$,

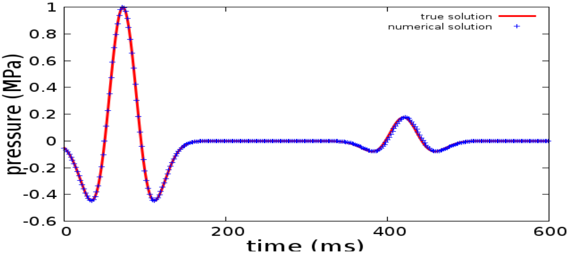

- first peak $\rightarrow$ trace of the direct wave
- second peak $\rightarrow$ trace of the reflected wave

Plane Wave: Ricker's wavelet

traces of the true and numerical solutions at 500 m, $h = 10$ m,

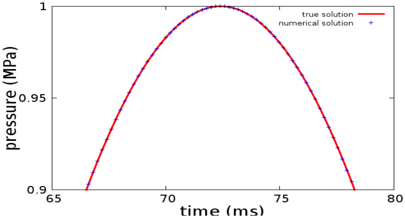

trace of the direct wave

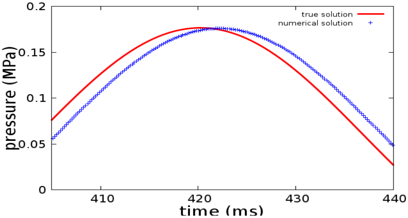

trace of the reflected wave

$$N = 4$$

Interface fitting Mesh Example

- using interface fitting mesh

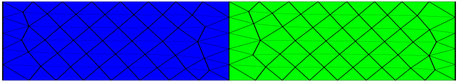

traces of the true and numerical solutions at 500 m, $h = 10$ m

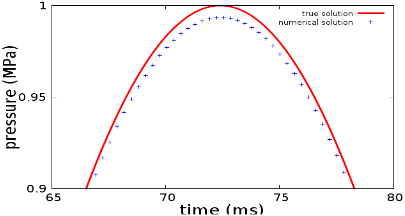

trace of the direct wave

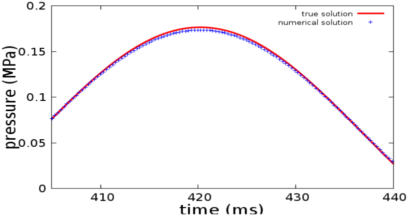

trace of the reflected wave

$N = 1$

Interface fitting Mesh Example

- using interface fitting mesh

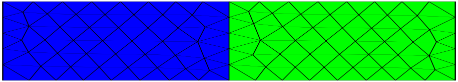

traces of the true and numerical solutions at 500 m, $h = 10$ m

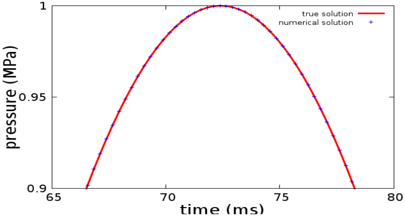

trace of the direct wave

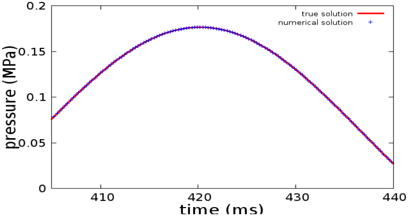

trace of the reflected wave

$N = 2$

Local Refined Mesh Example

- using local refined mesh grid

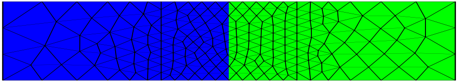

traces of the true and numerical solutions at 500 m, $h = 10$ m

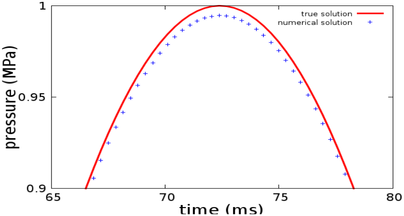

trace of the direct wave

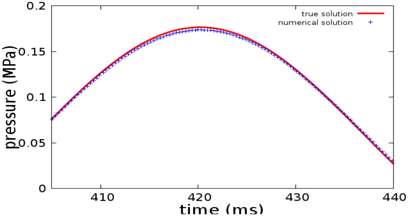

trace of the reflected wave

$N = 1$

Local Refined Mesh Example

- using local refined mesh grid

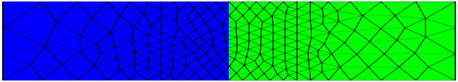

traces of the true and numerical solutions at 500 m, $h = 10$ m

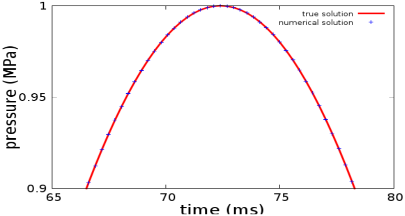

trace of the direct wave

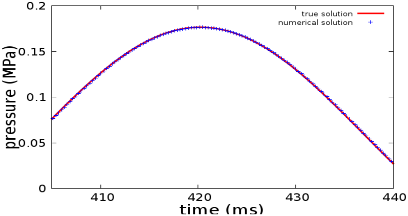

trace of the reflected wave

$N = 2$

Outline

Low-storage curvilinear DGTD

motivation

- DGTD on straight-sided eles $\Rightarrow$ a sub optimal 2nd order convergence rate when geometry representation not complement the accuracy of schemes
- applications with curvilinear geometry, e.g., material interfaces, boundaries
- DGTD has the flexibility to go beyond straight-sided eles

Curvilinear element

- straight-sided triangle T: $\forall \mathbf{x} \in T \Rightarrow$ the image of a point $(r, s) \in D = \{(r, s) | -1 \le r, s; r + s \le 0\}$ under the linear affine transform,

$$\mathbf{x} = -\frac{(r+s)}{2}\mathbf{x}_1 + \frac{(1+r)}{2}\mathbf{x}_2 + \frac{(1+s)}{2}\mathbf{x}_3$$

  $\mathbf{x}_i, i = 1, 2, 3$: vertices of T

- curvilinear triangle $\tilde{T}$: $\forall \mathbf{x} \in \tilde{T} \Rightarrow$ the image under an isoparametric transform

$$\mathbf{x} = \sum_j \mathbf{x}_j l_j(r, s)$$

  $\{l_j\}$: interpolating Lagrange polynomials on D
  $\{\mathbf{x}_j\}$: interpolating points on $\tilde{T}$

Steps to form curvilinear elements

reference: *Hesthaven and Warburton, '08*

- identify element edges that need to be curved
- reallocate the vertices and facial interpolating points on the curved material interfaces and/or boundaries
- blend the facial deformation on edges into the interior interpolating points through *Gordon-Hall* blending of face node deformation

  reference: *Gordon and Hall, '73*

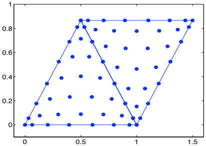

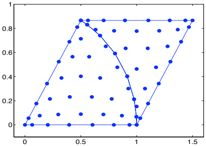

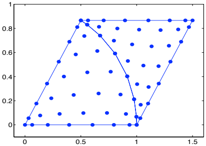

CurviDG formulation

numerical solutions on curvilinear element $\tilde{T}_k$

$$\mathbf{v}(\mathbf{x}(r,s),t)|_{\tilde{T}_k} = \sum_j \mathbf{v}_j^k(t) l_j(r,s)$$

$$p(\mathbf{x}(r,s),t)|_{\tilde{T}_k} = \sum_j p_j^k(t) l_j(r,s)$$

symmetric DG variational equations read

$$\rho_k \sum_j (l_i, l_j)_{\tilde{T}_k} \frac{\partial \mathbf{v}_j^k}{\partial t} = \sum_j (\nabla_{x,z} l_i, l_j)_{\tilde{T}_k}\ p_j^k - (l_i, \vec{n} p^*)_{\partial \tilde{T}_k}$$

$$\frac{1}{\kappa_k} \sum_j (l_i, l_j)_{\tilde{T}_k} \frac{\partial p_j^k}{\partial t} = -\sum_j (l_i, \nabla_{x,z} l_j)_{\tilde{T}_k} \cdot \mathbf{v}_j^k - (l_i, \vec{n} \cdot (\mathbf{v}^* - \mathbf{v}^-))_{\partial \tilde{T}_k}$$

Trouble for storage

the mass matrix M^k,

$$M_{ij}^k = \int_{\tilde{T}_k} l_i(r,s) l_j(r,s) \,\mathrm{d}x\,\mathrm{d}z = \int_D l_i(r,s) l_j(r,s) J^k(r,s) \,\mathrm{d}r\,\mathrm{d}s$$

the Jacobian $J^k(r,s) = \left| \dfrac{\partial \mathbf{x}}{\partial r} \times \dfrac{\partial \mathbf{x}}{\partial s} \right|$ is no longer constant,

- compute M_{ij}^k on the fly $\Rightarrow$ slowdown
- store M_{ij}^k $\Rightarrow$ storage scaled as $K_c \dfrac{(N+1)^2(N+2)^2}{4}$
  K_c: number of curvi eles
  $\dfrac{(N+1)(N+2)}{2}$: number of interp pnts

Weighting the variational spaces

weighting approximation space proposed by Warburton

$$V_h^J = \bigoplus_k \mathrm{span}\Big\{ \frac{l_j(r,s)|_{\tilde{T}_k}}{\sqrt{J^k(r,s)}} \Big\}$$

numerical solution in V_h^J

$$\mathbf{v}(\mathbf{x}(r,s),t)|_{\tilde{T}_k} = \sum_j \tilde{\mathbf{v}}_j^k(t) \frac{l_j(r,s)}{\sqrt{J^k(r,s)}}$$

$$p(\mathbf{x}(r,s),t)|_{\tilde{T}_k} = \sum_j \tilde{p}_j^k(t) \frac{l_j(r,s)}{\sqrt{J^k(r,s)}}$$

the mass matrix

$$M_{ij}^k = \int_D \frac{l_i(r,s)}{\sqrt{J^k}} \frac{l_j(r,s)}{\sqrt{J^k}} J^k(r,s) \, \mathrm{d}r \, \mathrm{d}s = \int_D l_i(r,s) l_j(r,s) \, \mathrm{d}r \, \mathrm{d}s = M_{ij}$$

$\Rightarrow$ without storage trouble

Low-storage curviDG

$$\rho_k \sum_j M_{ij} \frac{\partial \tilde{\mathbf{v}}_j^k}{\partial t} = \sum_j \left(\nabla_{x,z} l_i, l_j\right)_D \; \tilde{p}_j^k - \sum_j \left(l_i, \frac{l_j}{2} \nabla_{x,z} \log(J^k)\right)_D \tilde{p}_j^k - \left(\frac{l_i}{\sqrt{J^k}}, \mathbf{n}\tilde{p}^*\right)_{\partial \tilde{T}_k}$$

$$\frac{1}{\kappa_k} \sum_j M_{ij} \frac{\partial \tilde{p}_j^k}{\partial t} = -\sum_j (l_i, \nabla_{x,z} l_j)_D \cdot \tilde{\mathbf{v}}_j^k + \sum_j \left(l_i, \frac{l_j}{2} \nabla_{x,z} \log(J^k)\right)_D \cdot \tilde{\mathbf{v}}_j^k - \left(\frac{l_i}{\sqrt{J^k}}, \mathbf{n} \cdot (\tilde{\mathbf{v}}^* - \tilde{\mathbf{v}}^-)\right)_{\partial \tilde{T}_k}$$

e.g.,

$$\left(l_i, \frac{l_j}{2} \nabla_{x,z} \log(J^k)\right)_D = \sum_n \omega_i^c l_i(r_n^c, s_n^c) l_j(r_n^c, s_n^c) \nabla_{x,z} \log(J^k)(\mathbf{x}(r_n^c, s_n^c))$$

$\{(r_n^c, s_n^c)\}_n$, $\{\omega_n^c\}_n$: cubature nodes and weights on the reference element D

Outline

Square-circle model

nodal distribution of curvi eles of degree 8 near the circular region

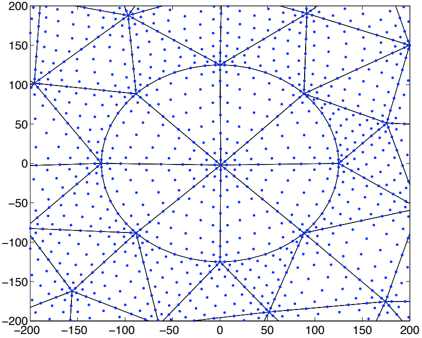

Square-circle model

- curvilinear DG, N=8 ⇒ optimal convergence rate

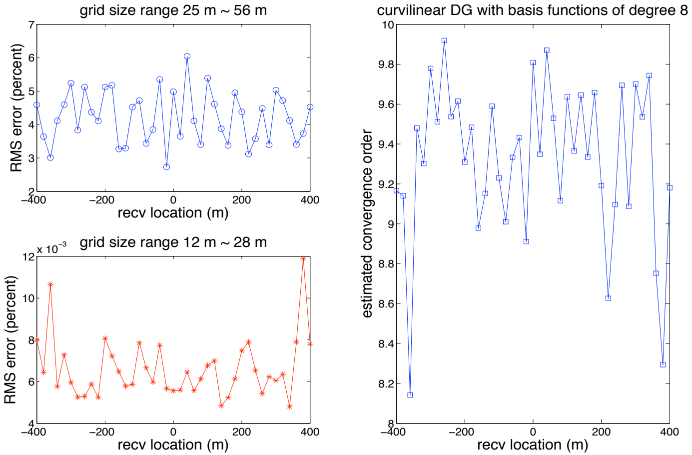

2D dome model

- 301 receivers at the depth 20 m with offset 100 $\sim$ 6100 m at interval 20 m
- point source with Ricker pulse at (3300 m, 40 m)
- curvilinear DG, N=5 $\Rightarrow$ almost optimal convergence rate except the boundary and the source nearby

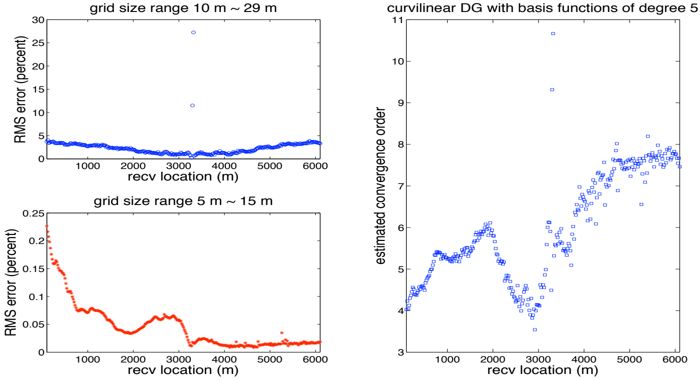

Outline

Summary

general realization:

- staggered-grid FDTD + interface error $\Rightarrow$ 1st order convergence rate
- DGTD, $N > 1$ + 'good' mesh $\Rightarrow$ 2nd convergence rate (sub-optimal)
- curviDG + 'perfect' mesh $\Rightarrow$ optimal convergence rate

Summary

comparison observation:

- FDTD for 'simple' models well resolves the interface error with less computation cost, e.g., square-circle model

- high order DGTD schemes have substantial advantage on 'complex' models and large time span, e.g., 2D dome model

- realistic models: need to explore for DGTD with advanced techniques, e.g.,
  - mesh generation from models defined on Cartesian grid
  - local mesh refinement + local time stepping

Future plan

- linear elastic wave equations
- seismic interface problems,
  e.g., water (acoustic) and solid (elastic) interface
- effective and efficient numerical methods for these problems,
  e.g., FD, FEM/DG

Thank You

Q&A